

BROADER PERSPECTIVES

Sun-trackers profitability analysis in Spain

Miguel de Simón-Martín¹*, Cristina Alonso-Tristán² and Montserrat Díez-Mediavilla²¹ E.I.I.I. León University, Campus of Vegazana s/n, 24071 León, Spain² Solar and Wind Feasibility Technologies E.P.S. Burgos University Campus of Río Vena, Avda. Cantabria s/n, 09006 Burgos, Spain

ABSTRACT

The principal objective of this study is to analyze the performance of sun-trackers devices compared with fixed flat plate systems using data from a widely used irradiation prediction software (PVGIS). We analyze typical parameters as daily and monthly sum of global irradiation (H_d and H_m) or average daily and monthly estimated electricity production (E_h and E_m) and also their associated costs and land requirements (usually described by the ground cover ratio, GCR). It was observed that the influence of these two last parameters is quite important to the calculation of the payback time of the whole installation. As a final result, it is concluded that although the dual-axis tracker allows the maximum energetic performance, a 38% higher than a fixed system on average, if we take into account the GCR value and calculate the surface performance ratio, the most efficient configuration is the horizontal-axis solar tracker. Copyright © 2013 John Wiley & Sons, Ltd.

KEYWORDS

photovoltaic panel tilting; sun-tracker; PVGIS; payback time; GCR ; SPR ; EPH

*Correspondence

Miguel de Simón-Martín, E.I.I.I. León University, Campus of Vegazana s/n, 24071 León, Spain.

E-mail: miguel.simon@unileon.es

Received 10 February 2012; Revised 14 September 2012; Accepted 14 November 2012

1. INTRODUCTION

A solar tracker is a machine that is designed as a mounting for photovoltaic panels so that they track the sun in such a way that the panels are perpendicular at most part of time to its rays, thereby increasing energetic production with respect to fixed systems [1]. Although using sun-tracking is not essential, its use can boost the collected energy in different periods of time and geographical conditions [2,3]. Many types of solar trackers exist, which vary in terms of cost, complexity and functions. They can also have varying degrees of precision according to their intended use.

Currently, several types of trackers are offered [4]. We can classify the sun tracker mechanisms according to the following:

- its control system,
- the movements they perform.

According to the control system, sun trackers can be mainly classified as [5]

- (i) active controlled sun-trackers,

- (ii) passive controlled sun trackers.

The active controlled sun trackers use motors and mechanical systems to transmit to the sun tracker the correct movements for sun tracking. These systems are precise, but, on the other hand, they are complex and with high rates of maintenance. Their associated costs are related with their precision accuracy.

The passive controlled sun trackers can be based on memory shape alloys or, more often, in the use of two cylinders and a liquefied gas with a low ebullition point. A pressure increment generated by the sun heating transfers the gas from a cylinder to the other one. This effect allows the mechanism the sun tracking. These kinds of systems are quite imprecise and not appropriate for certain applications (as for example concentration photovoltaics systems) [1].

On the other hand, the different models of trackers can be classified according to the movements they perform, in the following way [6]:

- (i) *Single-axis polar-mount trackers*. This kind of trackers are devices with a fixed N–S axis set at an

appropriate tilt angle (normally close to the latitude of the installation site), which acts as the rotation axis of the photovoltaic panels, so that they track the daily course of the sun [7].

- (ii) *Horizontal-axis trackers.* They have a horizontal axis that acts as a pivot for the panels, thereby allowing seasonal tracking of the sun.
- (iii) *Vertical-axis or azimuth sun trackers.* In this case, the panel array rotates about a fixed vertical axis for daily tracking [7].
- (iv) *Dual-axis sun trackers.* These devices offer better performance by enabling daily (E–W) and seasonal (N–S) solar tracking. They can be based on different configurations: polar-mount, rotating platform or parallel kinematics.

Of particular interest in this study, according to [8], is that more than 1/3 of the installations analyzed have sun tracking: 24% have dual-axis tracking and 13% have single-axis tracking. The rest are fixed systems.

Nowadays, the use of sun-tracking devices is rising because of the concentrating photovoltaic (CPV) technology, which requires a high-precision tracking of the sun [9]. High-concentration systems ($C > 100\times$)[†] require two-axis tracking with high precision (tolerances below 0.28 degrees) [10]. This kind of systems are intended to be based on Fresnel lenses, on Cassegrain Optics or on Light-guide Solar Optics systems (Figure 1). Medium concentration systems ($10\times < C < 100\times$) can generally be divided into two groups: parabolic troughs and those using Fresnel optics in the form of lenses or mirrors. They can use dual-axis tracking or one-axis tracking, if they are linear devices. Finally, low concentration systems ($C < 10\times$) fall an extremely large number of devices and variations based on very distinct technologies. In most cases, they are static or with one-axis tracking [10,11].

2. MATERIAL AND METHODS

To estimate the performance of the different types of mechanisms in Spain, we have analyzed the results of the Photovoltaic Geographical Information System (PVGIS) estimation utility [12] for the six different locations shown in Figure 2.

These locations has been selected due to its geographic distribution and different values of solar irradiation, as it is shown in Figure 3.

Several commercially available as well as free downloadable prediction software tools exist. These software tools can be used to calculate the energy production of a desired system by simply computing the system sizing parameters. The most commonly used models for

[†] Factor C is the ratio between the aperture area of the primary concentrator and the active cell area. $C = 2\times$ means that the aperture area doubles the active cell area.

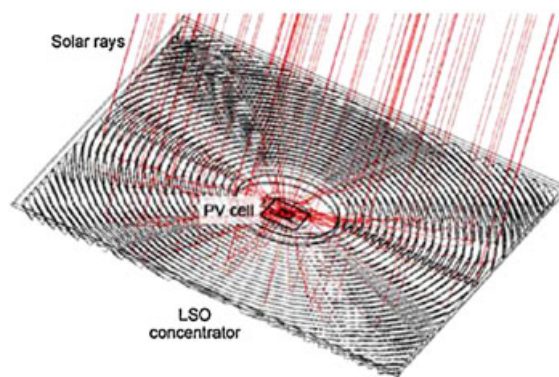


Figure 1. Example of a concentrating photovoltaic system based on a Fresnel lens. Source: [10].

predicting the performance of grid-connected and residential PV systems are: PVWATTS, PVSYST, System Advisor Model (SAM), MAUI, RETSCREEN and PVGIS [14,15]. A quick overview of these models is presented hereafter.

The PVWATTS is a web based software model that calculates electrical energy produced by a grid-connected PV system. This model was developed by the Renewable Resource Data Center, which is supported by the National Center for Photovoltaics in the USA. The PVWATTS model uses a 30-year average daily weather data from different places in the USA to determine the daily amount of solar energy (insolation), and uses it to calculate the amount of energy a system will produce on the basis of the systems configuration [16].

The PVSYST software is a European based PV system predictor developed by the University of Geneva for the European Center of Energy. This PC software package is suitable for studying, simulating and analyzing PV systems. The software is suitable for both stand-alone and grid-connected PV systems [17].

The System Advisor Model (SAM) was developed in 1996 by The National Renewable Energy Laboratory (NREL) in the USA, jointly with Sandia National Laboratory and in partnership with the US Department of Energy (DOE) Solar Energy Technologies Program (SETP). The SAM is able to evaluate several types of financing (from residential to utility-scale) and a variety of technology-specific cost models for several renewable technologies. This software is widely used because of its great database [18].

The MAUI solar modeling software program has a climate database of 239 locations in the continental US, Alaska, Hawaii, Puerto Rico, and Guam. It is also capable of generating worldwide hourly climate generation with 2 132 international climates database that compiles any of the climates for use with the program. Users can choose preset climates or create own climate files based on user-defined data available for a particular site [19].

The RETSCREEN program is used in 222 countries by about 136 000 users. It is capable of determining energy productions, savings, life-cycle costs, emissions reduc-



Figure 2. Studied locations in Spain. Adapted from Google Earth App.

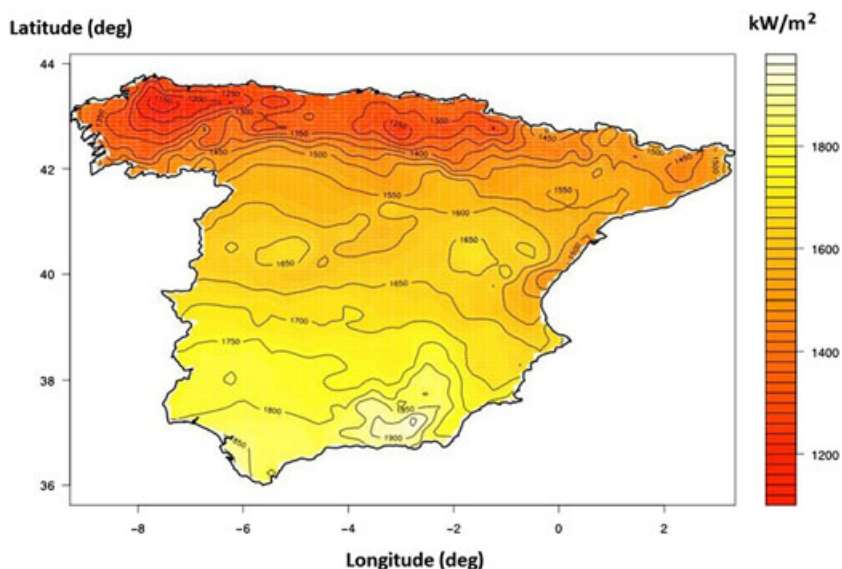


Figure 3. Horizontal radiation in Spain. Source: [13].

tions, and energy production from multiple sources other than PV [20].

The PVGIS incorporates a solar radiation database and gives climatological data of Europe. This system makes it possible to calculate long-term average values and daily profiles of the irradiation on PV modules [21]. The PVGIS estimates have been widely used by developers to compare energy production between fixed and tracking installations [22].

The main characteristics of the previous programs have been summarized in Table I.

Due to the simplicity and extended use of PVGIS, we use it here to calculate the theoretical achievable energy production for different PV configurations. It offers enough accuracy for carrying out the study [23].

The PVGIS needs data on solar radiation in order to make estimates of the performance of PV systems and to do the other calculations possible in the web application.

Table I. Irradiation prediction softwares comparison.

| Software | License | Application | Accuracy |
|-----------|-----------|----------------------------|---------------------|
| PVWATTS | Free | Worldwide | Medium |
| PVSYST | Shareware | Worldwide | Depends on database |
| SAM | Free | Worldwide (preferably USA) | Depends on database |
| MAUI | Private | North America | Very high |
| RETSCREEN | Free | Worldwide | High |
| PVGIS | Free | Europe and Africa | High |

There exist a number of different sources of solar radiation data, but none of them are perfect, so it is important to understand the strengths and weaknesses of each data source. In the new version of PVGIS (autumn 2010), it included a choice of solar radiation databases for some regions [22]. The two main sources of data on solar radiation at the surface of the earth are as follows:

- ground measurements,
- calculations based on satellite data.

Direct measurements of the solar radiation at ground level can be made with a number of different instruments. One widely used instrument is the pyranometer. Typically, this instrument measures all the radiation coming from the sun and from the sky or clouds. When you want to know the solar radiation at a specific place, ground station measurements give the best results. It is also possible to measure with a high time resolution, typically every minute or even more often.

Possible problems with the measurements, apart from failure in the measurement system itself, is that the sensor may be covered with dirt, frost, or snow, or that the sensor is shadowed by nearby trees or buildings for some of the time during the year.

When there are no direct measurements at a given place, it is still possible to estimate the solar radiation from measurements made nearby. Of course, the quality of the estimate will decrease as the distance to the measurement site increases. It is also possible to combine data from several different measurement locations to make an estimate for the solar radiation in a place somewhere between the measurement sites. This method was used in the original PVGIS solar radiation database for Europe.

There are a large number of methods to estimate the solar radiation at ground level using data sets from satellites. Typically the satellites measure the light (visible or infrared) coming from the Earth. This light is mainly the light reflected from the ground or from clouds. The calculation of the solar radiation at ground level must therefore be able to take into account the radiation absorbed by the atmosphere as well as that reflected by clouds.

The new CM-SAF-PVGIS database for Europe and Northern Africa is based on calculations from satellite images performed by CM-SAF. The database represents a total of 12 years of data. From the first generation of Meteosat satellites, known as MFG, there are data from

1998 to 2005 and from the second-generation Meteosat satellites (known as MSG) and there are data from June 2006 to May 2010 [24].

In this case, we preferred the new CM-SAF-PVGIS database because it represents better results for the cases we studied.

The parameters used in the PVGIS for each case study are the same, and they are shown in Table II. Although the PVGIS allows the user to simulate different PV technologies, in this case we have used the Unknown/Other option because it provides the most conservative solution.

To simulate the PV energy production for a fixed system, we optimized the azimuth angle (0° South) and the slope of the tilting surfaces for each location. For dual-axis tracking, we set the optimum values for both angles automatically. For vertical and inclined axis or polar tracking, we also have optimized the slope angle. The PVGIS system does not allow the user to simulate a horizontal-axis tracker directly. For that case we simulated the installation as a fixed one with different tilting angles from 15° to 75° with 10° step. Then, we have used the best results for each month of the year obtained in Table III and can be mathematically demonstrated with expression (1), which obtains the zenith angle of the sun (σ_Z) [2]. The optimum slope angles for most studied locations are shown in Figure 4.

$$\cos(\sigma_Z) = \sin(\phi) \sin(\delta) + \cos(\phi) \cos(\delta) \cos(\omega) \quad (1)$$

where ϕ is the geographical latitude (positive sign for the North), δ is the declination, which depends on the day of the year (Equation (2)), and ω is the hourly angle, which expresses the sun hour in angle values.

$$\delta = 23.45 \sin\left(360 \frac{284 + N}{365}\right) \quad (2)$$

where N is the day of the year.

Figure 4 is near symmetric and shows that the optimum angle in winter is about 65° , and in summer, its value is close to 15° .

3. RESULTS

In this section, we are going to compare the performance ratios between the different sun trackers classified in Section 1 according to their movement.

Table II. The PVGIS parameters.

| Parameter | Value |
|-------------------------|---------------|
| PV technology | Unknown/Other |
| Peak PV power | 1 kWp |
| Estimated system losses | 14% |

Table III. Study of the optimum tilting angle. Values in the table are the simulated mean of global irradiation [kWh/m²] for the studied location for each month of the year and each angle from 15° to 75° with variations of 10°.

| Month | 15° | 25° | 35° | 45° | 55° | 65° | 75° | Max | Optimum |
|---------|-------|-------|-------|-------|-------|-------|-------|-------|---------|
| Jan | 60.3 | 67.8 | 73.8 | 78.0 | 80.3 | 80.7 | 79.0 | 80.7 | 65 |
| Feb | 83.8 | 92.2 | 98.4 | 102.0 | 104.0 | 102.0 | 98.5 | 104.0 | 55 |
| Mar | 138.0 | 146.0 | 152.0 | 153.0 | 151.0 | 145.0 | 136.0 | 153.0 | 45 |
| Apr | 155.0 | 158.0 | 157.0 | 153.0 | 145.0 | 134.0 | 119.0 | 158.0 | 25 |
| May | 193.0 | 191.0 | 185.0 | 175.0 | 161.0 | 144.0 | 123.0 | 193.0 | 15 |
| Jun | 217.0 | 212.0 | 202.0 | 188.0 | 169.0 | 147.0 | 123.0 | 217.0 | 15 |
| Jul | 235.0 | 231.0 | 221.0 | 207.0 | 187.0 | 163.0 | 136.0 | 235.0 | 15 |
| Aug | 211.0 | 213.0 | 211.0 | 203.0 | 190.0 | 172.0 | 150.0 | 213.0 | 25 |
| Sep | 166.0 | 175.0 | 179.0 | 179.0 | 175.0 | 165.0 | 152.0 | 179.0 | 35 |
| Oct | 111.0 | 121.0 | 128.0 | 132.0 | 133.0 | 130.0 | 124.0 | 133.0 | 55 |
| Nov | 72.1 | 81.1 | 88.2 | 93.2 | 95.8 | 95.9 | 93.6 | 95.9 | 65 |
| Dec | 58.8 | 67.6 | 74.8 | 80.2 | 83.5 | 84.7 | 83.7 | 84.7 | 65 |
| Average | 141.7 | 146.3 | 147.5 | 145.3 | 139.5 | 130.3 | 118.1 | 153.9 | 40 |

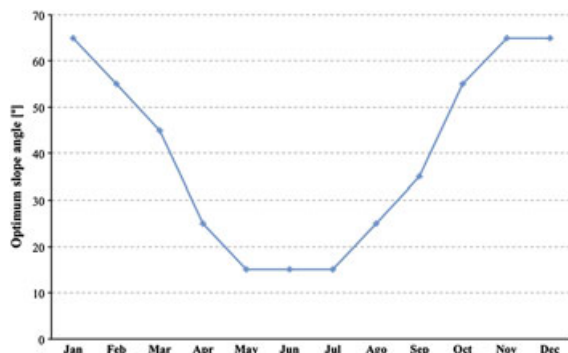


Figure 4. Optimum slope angles for most locations.

3.1. Location differences

First of all, we have to analyze if there are too many differences between the results from one location and another. Table IV shows the standard deviations of the studied parameters referred to the average value taken into account for the other analysis. In this case, we can take the average value and generalize the results to the whole Spanish territory, because the standard deviations are small (less than 10%). However, for most accurate studies, we have to take this fact into account, and the results must be reviewed.

In Table IV *Ed* is the average daily electricity production, *Em* is the average monthly electricity production, *Hd* is the average daily sum of global irradiation and *Hm* is the average monthly sum of global irradiation.

3.2. Production analysis

Table V shows the average daily sum of global irradiation on a fixed system and the increased performance for each solar tracker system. We can conclude that the more efficient system is the dual-axis sun tracker with 38.43% better performance ratio than a fixed system. On the other hand, the horizontal axis sun tracker only improves by 5.87%. Results can be compared in Figure 5.

Table VI shows another important parameter: the average monthly electricity production for a fixed system and the increased performance for each sun-tracker system. We notice that results are quite slightly different from the *Hd* parameter. Nevertheless, the dual-axis system still achieves the best performance, 38.01% better than a fixed system. The horizontal-axis system is also the worst tracker, but improves by 6.12% of the energy production. Results for the whole year can be compared also in Figure 6.

It is important to notice that the increased performances among a vertical-axis sun tracker, polar-mount sun tracker and dual-axis sun tracker are very close.

Figure 7 shows the increased performance for each system, taking into account the average monthly electricity production.

We also can analyze the performance for each month of the year in Figure 8. In this figure, we notice that the performance ratio increases at most in summer for all sun-tracking systems, specially for the dual-axis sun tracker. For that system, the performance in June can be 56.08% higher than a fixed system. On the other hand, in January, the performance only increases 29.67%. The vertical-axis

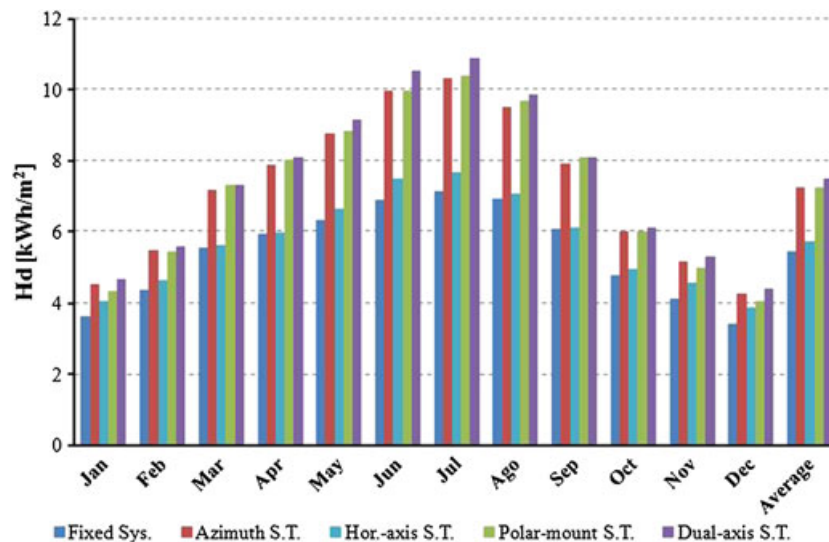
Table IV. Standard deviation for each analyzed parameter.

| Parameter | Fixed sys. [%] | Vert. S.T. [%] | Hor. S.T. [%] | Polar S.T. [%] | Two-axis S.T. [%] |
|-----------|----------------|----------------|---------------|----------------|-------------------|
| <i>Ed</i> | 8.06 | 8.55 | 8.51 | 8.60 | 8.82 |
| <i>Em</i> | 8.05 | 8.55 | 8.51 | 8.59 | 8.80 |
| <i>Hd</i> | 7.98 | 8.45 | 8.40 | 8.50 | 8.75 |
| <i>Hm</i> | 7.97 | 8.47 | 8.38 | 8.48 | 8.71 |
| Average | 8.01 | 8.50 | 8.45 | 8.54 | 8.77 |

Note: *Ed*, average daily electricity production; *Em*, average monthly electricity production; *Hd*, average daily sum of global irradiation; *Hm*, average monthly sum of global irradiation.

Table V. Increased performance in the average daily sum of global irradiation between the different sun-tracker systems (*Hd*).

| Month | Fixed [kWh] | Vert. S.T. [%] | Hor. S.T. [%] | Polar S.T. [%] | Two-axis S.T. [%] |
|---------|-------------|----------------|---------------|----------------|-------------------|
| Jan | 3.63 | 24.67 | 11.85 | 19.80 | 28.43 |
| Feb | 4.39 | 25.27 | 5.85 | 23.97 | 27.74 |
| Mar | 5.57 | 29.15 | 0.87 | 31.22 | 31.61 |
| Apr | 5.94 | 32.58 | 0.65 | 35.42 | 36.40 |
| May | 6.32 | 38.59 | 5.40 | 39.85 | 44.86 |
| Jun | 6.88 | 44.89 | 8.79 | 44.75 | 53.03 |
| Jul | 7.15 | 44.55 | 7.42 | 45.42 | 52.30 |
| Ag | 6.94 | 36.88 | 1.90 | 39.74 | 41.99 |
| Sep | 6.10 | 29.99 | 0.03 | 32.50 | 32.53 |
| Oct | 4.79 | 25.76 | 3.41 | 25.76 | 27.88 |
| Nov | 4.13 | 25.06 | 10.21 | 21.19 | 28.49 |
| Dec | 3.42 | 24.85 | 14.08 | 18.86 | 29.53 |
| Average | 5.44 | 31.85 | 5.87 | 33.64 | 38.03 |

**Figure 5.** Average daily sum of global irradiation.

and polar-mount sun trackers have similar behaviors as the dual-axis sun tracker. However, the horizontal-axis sun tracker improves its performance in summer and winter near by 12–15%, but in spring and autumn, it has near the same performance as a fixed system, because the inclined angle is the same.

3.3. Surface performance ratio

Table VII analyzes what happens if we take into account the surface needed for each sun-tracker system. The area occupied for each system has been estimated, according to the shadows generated in a horizontal land and the

Table VI. Increased performance in the average monthly electricity production between the different sun-tracker systems (*E_m*).

| Month | Fixed [kWh] [%] | Vert. S.T. [%] | Hor. S.T. [%] | Polar S.T. [%] | Two-axis S.T. [%] |
|---------|-----------------|----------------|---------------|----------------|-------------------|
| Jan | 86.00 | 25.83 | 12.54 | 20.68 | 29.67 |
| Feb | 93.87 | 26.15 | 6.14 | 24.68 | 28.75 |
| Mar | 131.33 | 30.71 | 0.89 | 32.74 | 33.25 |
| Apr | 135.17 | 34.65 | 0.62 | 37.48 | 38.22 |
| May | 148.33 | 40.90 | 5.51 | 42.25 | 47.42 |
| Jun | 156.33 | 47.44 | 9.17 | 47.44 | 56.08 |
| Jul | 168.00 | 46.83 | 7.64 | 48.02 | 55.16 |
| Ag | 163.33 | 38.98 | 2.14 | 42.04 | 44.08 |
| Sep | 139.50 | 31.54 | -0.12 | 33.93 | 34.29 |
| Oct | 113.40 | 26.84 | 3.47 | 26.84 | 29.04 |
| Nov | 94.82 | 26.12 | 10.62 | 22.11 | 29.51 |
| Dec | 81.05 | 26.05 | 14.83 | 19.56 | 30.68 |
| Average | 125.93 | 33.50 | 6.12 | 33.15 | 38.01 |

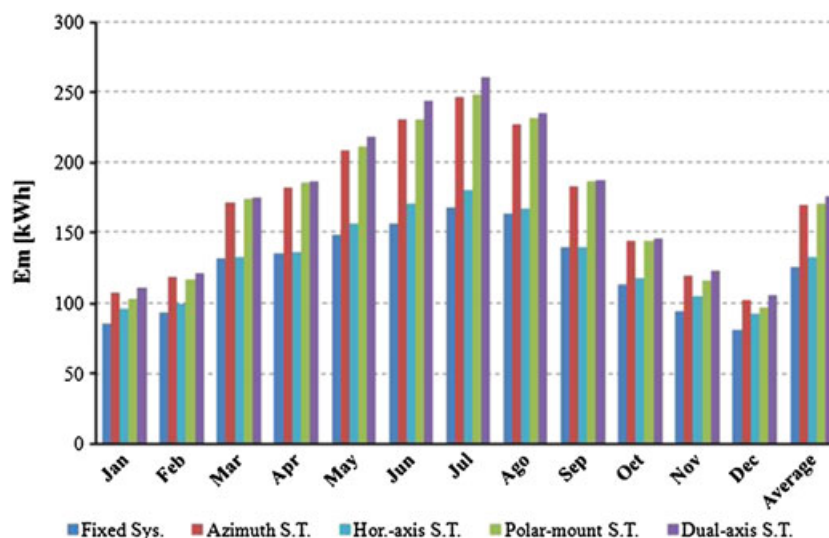


Figure 6. Average monthly electricity production.

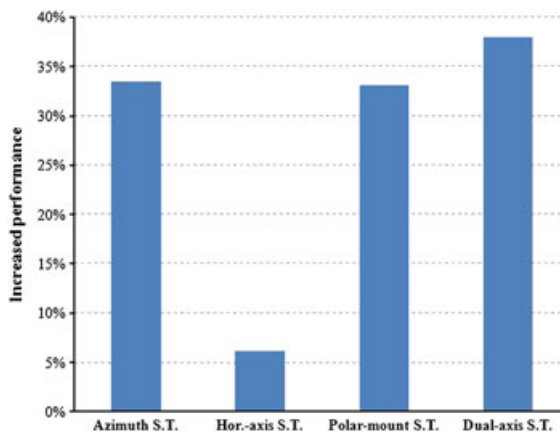


Figure 7. Increased performance in average monthly electricity production.

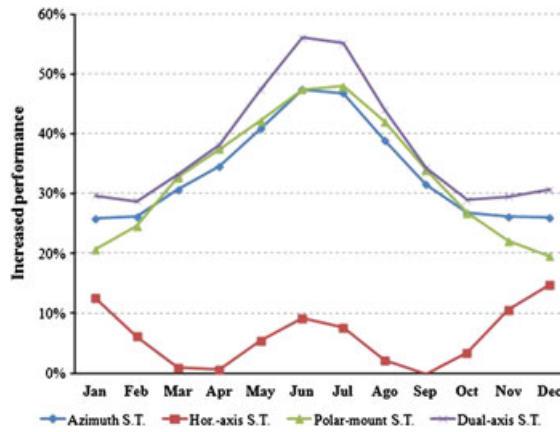


Figure 8. *E_m* increased performance ratio for each month.

Table VII. Increased surface performance from fixed systems.

| Tracker | Shadows [%] | Area [m ²] | kWp/m ² | Energy [kWh] | kWh/m ² |
|---------------|-------------|------------------------|--------------------|--------------|--------------------|
| Fixed system | 0.50 | 14 600 | 0.0682 | 1 503 578 | 103.0 |
| Azimuth S.T. | 3.00 | 24 500 | 0.0396 | 1 981 274 | 80.9 |
| Hor-axis S.T. | 0.50 | 14 600 | 0.0682 | 1 586 395 | 108.7 |
| Polar S.T. | 3.00 | 25 900 | 0.0375 | 1 985 105 | 76.6 |
| Two-axis S.T. | 3.00 | 49 400 | 0.0196 | 2 178 708 | 44.1 |

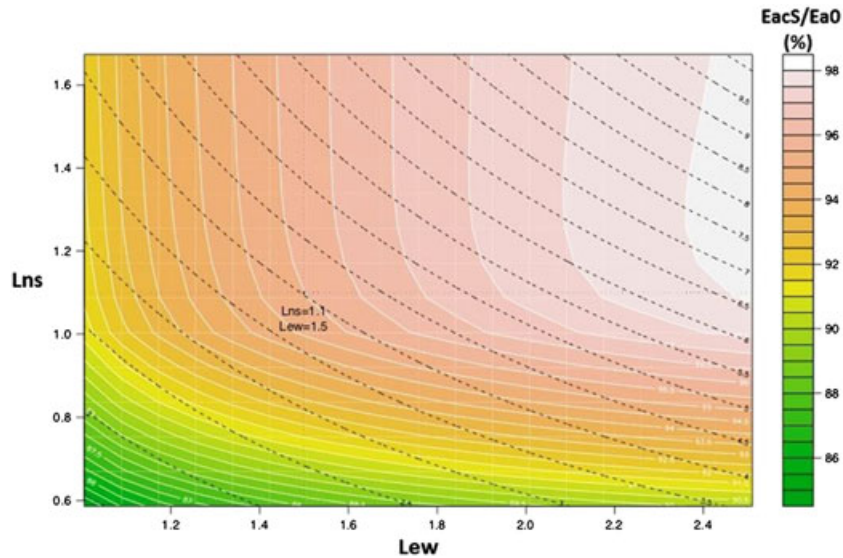


Figure 9. Shadows between dual-axis trackers ($b = 0.475$). Source: [13].

limited tracking angle [13,25,26]. Figure 9 is an abacus to calculate the North–South distance (L_{ns}) and the East–West distance (L_{ew}) between dual-axis trackers with an aspect ratio $b = 0.475$ (length/width of the PV array). The theoretical values match with those from known real installations.

Some authors use a specific parameter called ground cover ratio (GCR) [27,28], which is defined as the ratio of

the PV array area (S_{pv}) to total ground area for the system (S_{ground}), as it is shown in Equation (3).

$$GCR = \frac{S_{pv}}{S_{ground}} \tag{3}$$

However, we use an equivalent but more representative parameter called surface performance ratio (SPR). This has

been defined as the ratio of the energy produced (E) and ground area occupied by the system (4). Both parameters are directly proportional to the installed peak power.

$$SPR = \frac{E}{S_{\text{ground}}} \quad (4)$$

In this case, and as it is represented in Figures 10 and 11, the better system is the horizontal-axis sun tracker, because it needs about the same area as a fixed system but increases the energy production. The worst system from this point of view is the dual-axis sun tracker because it generates a lot of shadows and so, it needs large distances between each device.

Table VIII compares the performance ratios for each system taking into account only the energy production or considering also the installation surface needed.

3.4. Payback time analysis

We finally analyzed the payback time for each installation, taking into account both performance ratios described

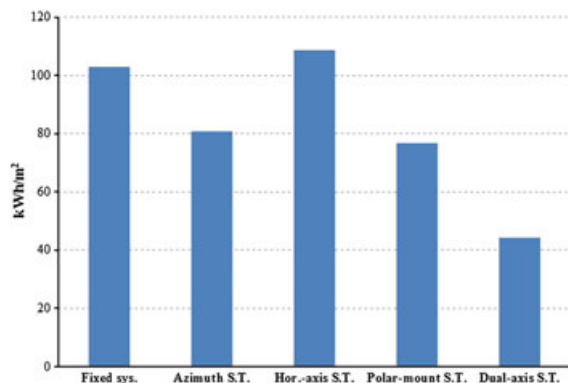


Figure 10. Surface production for each technology.

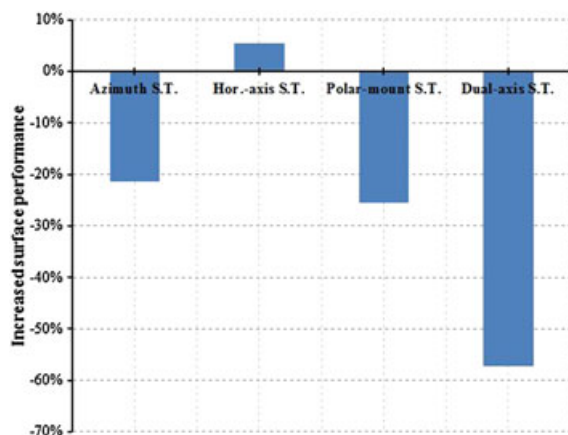


Figure 11. Increased surface performance with respect to a fixed system.

Table VIII. Increased performance ratios from a fixed system.

| Tracker | Inc. perf. [%] | Inc. surf. perf. [%] |
|----------------|----------------|----------------------|
| Azimuth S.T. | 33.5 | -21.5 |
| Hor.-axis S.T. | 6.1 | 5.5 |
| Polar S.T. | 33.2 | -25.6 |
| Two-axis S.T. | 38.0 | -57.2 |

Table IX. Payback time analysis.

| Tracker | Cost [eur/kWp] | PR 1 | PR 2 |
|-------------|----------------|------|------|
| Fixed sys. | 1 450.00 | 1.00 | 1.00 |
| Vert. S.T. | 2 015.17 | 1.05 | 1.77 |
| Hor. S.T. | 2 165.67 | 1.41 | 1.41 |
| Polar S.T. | 2 140.29 | 1.12 | 1.98 |
| 2-axis S.T. | 2 228.65 | 1.09 | 3.68 |

before. To do this, we have collected information for the average cost of each sort of sun tracker from the manufacturers and installers [4] and compared it with the cost that a fixed system involves [29]. The results are shown in Table IX (where PR 1 is the payback ratio considering the energy production ratio and PR 2 is the payback ratio considering the surface performance ratio) and also in Figures 12 and 13. The payback ratio is calculated with the expression (7).

$$FPT = \frac{i + i_f}{c \cdot p_f} \quad (5)$$

FPT is the payback time for fixed systems measured in years, where i is the inversion costs of the installation except the mounting structure in euros, i_f is the cost of the mounting structure in euros, c is the retribution of the produced energy in euros/kWh and p is the yearly energy production in kWh/year.

$$TPT = \frac{i + i_t}{c \cdot p_t} \quad (6)$$

TPT is the payback time for tracker systems measured in years, where i_t is the cost of the tracker device measured in euros.

$$PR = \frac{TPT}{FPT} = \frac{\frac{i+i_t}{c \cdot p_t}}{\frac{i+i_f}{c \cdot p_f}} = \frac{i + i_t}{i + i_f} \cdot \frac{p_f}{p_t} \quad (7)$$

There is a big difference if we take into account the simple energy production performance ratio or if we consider the surface performance ratio. In the first case, a dual-axis sun-tracking system only needs a 0.09 times larger payback time than a fixed system, but in the second case, the same system needs a 2.68 times larger payback time. On the other hand, a horizontal-axis sun tracker has a 41% larger payback time for both cases.

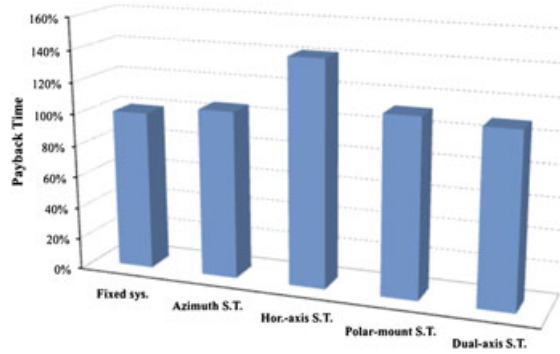


Figure 12. Payback time comparison taking into account the energy production ratio.

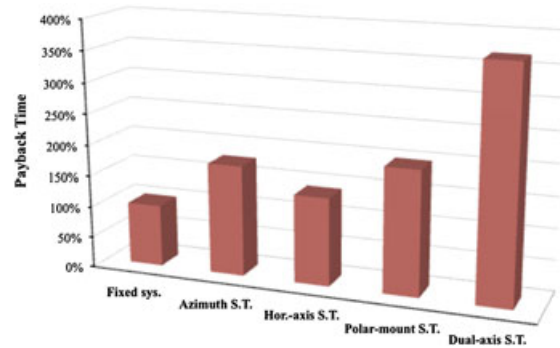


Figure 13. Payback time comparison taking into account the surface performance ratio.

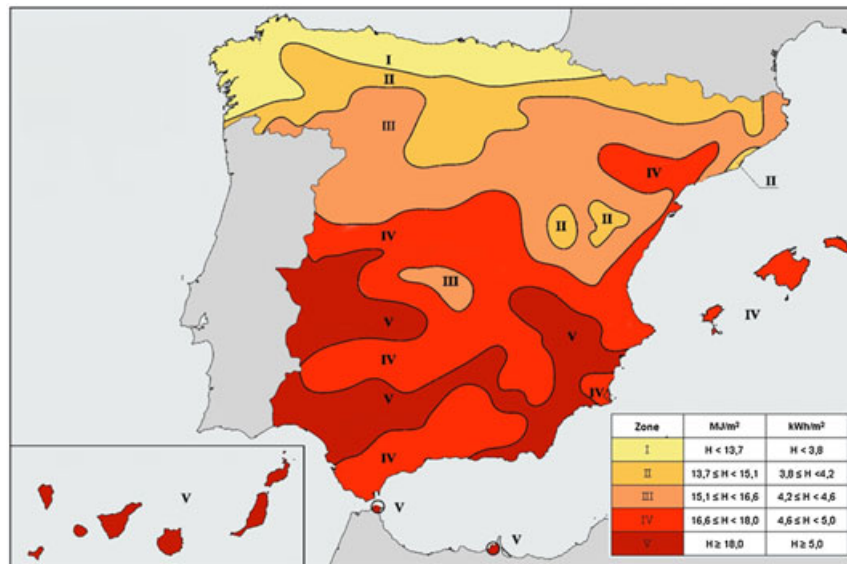


Figure 14. Spanish photovoltaic zones, where H is the horizontal global radiation. Source: [30].

3.5. Equivalent production hours

We have considered it is important to know the concept of equivalent production hours (EPH) mentioned on the latest

Spanish PV regulation [30]. This law established a maximum limit of production for each type of technology and geographical location of the installation. Figure 14 shows the five areas in which the spanish territory has been divided according to its photovoltaic potential.

Table X. Comparison of the *HEQ* values for PV estimations and the maximum limit.

| Zone | Fixed Syst. | One-axis S.T | Two-axis S.T. |
|----------------|-------------|--------------|---------------|
| Zone I | 1 232 | 1 602 | 1 664 |
| PV est. I | 1 348 | 1 825 | 1 882 |
| Error I [%] | 9.38 | 13.95 | 13.09 |
| Zone II | 1 362 | 1 770 | 1 838 |
| PV est. II | 1 345 | 1 801 | 1 854 |
| Error II [%] | -1.27 | 1.73 | 0.85 |
| Zone III | 1 492 | 1 940 | 2 015 |
| PV est. III | 1 539 | 2 059 | 2 130 |
| Error III [%] | 3.17 | 6.13 | 5.71 |
| Zone IV | 1 632 | 2 122 | 2 204 |
| PV est. IV | 1 570 | 2 144 | 2 220 |
| Error IV [%] | -3.83 | 1.04 | 0.73 |
| Zone V | 1 753 | 2 279 | 2 367 |
| PV est. V | 1 650 | 2 262 | 2 343 |
| Error V [%] | -5.86 | -0.75 | -1.01 |
| Avg. Error [%] | 0.32 | 4.42 | 3.87 |

The *EPH* is defined as the ratio of the yearly energy production, measured in kWh (*E*), and the nominal power of the installation in kW (*P*), as it is shown in Equation (8).

$$EPH = \frac{E}{P} \quad (8)$$

This is a very important factor to calculate the real performance of our installations. If we produce more *EPH* than the maximum limit along the year, that production will not be supported by the Spanish Government (currently, since January 2012 the incentive payments are temporarily called off by RD-L 1/2012), and so, we will have to sell that energy in the Pull Market (at very low prices). Thus, we have to take into account that limit, and we should use the worst value between the PV estimation and the limit to calculate the real energy performance. Table X shows the comparison between the PV estimation with PVGIS and the regulation limit for each geographical area.

As shown in Table X, the PV production estimation used to obtain a higher *EPH* than the maximum regulated limit; so, we have to be aware of this, specially in analyzing the financial profitability of our installation. The maximum error achieves the 14% in some cases, and it is higher when we consider a tracking system.

4. CONCLUSIONS

There is not an ideal tracker device for all possible installation cases. Designers and engineers have to take into account the advantages and disadvantages from each tracking system. For not grid connected installations, domestic ones or power size less than 20 kWp a fixed system could be enough, but if we dispose of an installation of more than 100 kWp, we will be really interested in increasing the performance ratio, and we must install a tracking system to maximize the profit. In this case, we have to be aware of the surface performance ratio (*SPR*), which is

higher in horizontal-axis tracking systems as it has been demonstrated. These devices are also simple and easy to control and maintain [4].

On the other hand, if we have enough space or we face a CPV, the dual-axis tracking device allows us to achieve the best energy production performance ratio [31,32]. However, a well configured azimuth-axis or polar-mount sun tracker can achieve close results, and they are less complex devices. Azimuth tracking (included in the dual-axis solar trackers) is specially interesting in summer applications as can be seen in the production analysis results.

The ideal tracker device has anyway to be a simply assembled mechanism, which requires easy low-levels of maintenance.

It may be highlighted that the majority of applications developed to date are principally intended to be mounted on the ground. However, recent Spanish and European countries legislation on photovoltaic energy is restricting their expansion on the ground, and is leading to the development of smaller and more compact trackers that are adaptable to storage center or household rooftops, where the regulatory limitations are at present less restrictive [30,33].

Finally, we want to highlight the importance of taking into account the equivalent production hours (*EPH*) when we calculate the profitability of our installation. The error in real profitable production can achieve near the 14% in some cases and 3% on average. This fact will help us to optimize the configuration of our installations.

ACKNOWLEDGEMENTS

This research has received economic support from the Spanish Government (grant ENE2011-27511) and the Department of Culture and Education of the Regional Government of Castilla y León, Spain (grant BU358A12-2). Furthermore, M. de Simón-Martín is grateful for the FPU (Formación del Profesorado Universitario) programme.

REFERENCES

1. Mousazadeh H, Keyhani A, Javadi A, Mobli H, Abrinia K, Sharifi A. A review of principle and sun-tracking methods for maximizing solar systems output. *Renewable and Sustainable Energy Reviews* 2009; **13**(8): 1800–1818.
2. Iqbal M. *An Introduction to Solar Radiation*. Academic Press: California, USA, 1983. ISBN: 9780123737526.
3. Coffari E. *The Sun and the Celestial Vault*, Solar Energy Engineering. Academic Press: New York, 1977.
4. Siemer J, de Saravia CF. El éxito de la sencillez - Sistemas de seguimiento. *Revista Photón* 2011; **10**(September): 42–75.
5. Oner Y, Cetin E, Ozturk HK, Yilanci A. Design of a new three-degree of freedom spherical motor for photovoltaic-tracking systems. *Renewable Energy* 2009; **34**(12): 2751–2756.
6. de Simón-Martín M, Gómez-Gil FJ, Peláez-Vara J, Ruiz-Calvo J. A review of solar tracker patents in Spain. In *Proceedings of the 3rd WSEAS International Conference*, vol. 2, World Scientific, Engineering Academy, and Society (WSEAS) (eds), Energy Problems & Environmental Engineering. World Scientific Engineering Academy and Society (WSEAS): Sta. Cruz de Tenerife, Spain, 2009; 292–297. ISSN/ISBN: 1790-5095 / 978-960-474-093-2.
7. Huld T, Cebecauer T, Šúri M, Dunlop ED. Analysis of one-axis tracking strategies for PV systems in Europe. *Progress in Photovoltaics: Research and Applications* 2010; **18**(3): 183–194.
8. Hacia la consolidación de la energía solar fotovoltaica en España. *Informe Anual*, Asociación de la Industria Fotovoltaica (ASIF), 2009.
9. Ota Y, Nishioka K. Three-dimensional simulating of concentrator photovoltaic modules using ray trace and equivalent circuit simulators. *Solar Energy* 2012; **86**(1): 476–481.
10. Chemisana D. Building integrated concentrating photovoltaics: a review. *Renewable and Sustainable Energy Reviews* 2011; **15**(1): 603–611.
11. Baig H, Heasman KC, Mallick TK. Non-uniform illumination in concentrating solar cells. *Renewable and Sustainable Energy Reviews* 2012; **16**(8): 5890–5909.
12. PVGIS: PV potential estimation utility, Retrieved 05/11/11. <http://re.jrc.ec.europa.eu/pvgis/apps4/pvest.php>.
13. Perpiñán O. Grandes Centrales Fotovoltaicas: Producción, Seguimiento y Ciclo de Vida. *PhD. Thesis*, Universidad Nacional de Educación a Distancia (Spain), 2008.
14. Tamith-Mani G, Ishioye JP, Voropayev A, Kang Y. Photovoltaic performance models: an evaluation with actual field data. In *Proceedings of the SPIE 2008, Reliability of Photovoltaic Cells, Modules, Components and Systems*, Vol. 7048, Dhere NG (ed). Art. No.: 70480W. DOI: 10.1117/12.794245.
15. Connolly D, Lund H, Mathiesen BV, Leahy M. A review of computer tools for analysing the integration of renewable energy into various energy systems. *Applied Energy* 2010; **87**(4): 1059–1082.
16. PVWATTS: a performance calculator for grid-connected PV systems, Retrieved 05/12/12. <http://rredc.nrel.gov/solar/calculators/pvwatts/version1/>.
17. PVSyst: photovoltaic software, Retrieved 05/12/12. <http://www.pvsyst.com/en/>.
18. SAM: system advisor model, Retrieved 05/12/12. <https://sam.nrel.gov/>.
19. MAUI: energy software corporation, Retrieved 05/12/12. <https://sam.nrel.gov/>.
20. RETScreen, Retrieved 05/012/12. <http://www.retscreen.net/es/home.php>.
21. Šúri M, Huld TA, Dunlop ED. PV-GIS: a web-based solar radiation database for the calculation of PV potential in Europe. *International Journal of Sustainable Energy* 2005; **24**(2): 55–67, ISBN: 1478646X.
22. Šúri M, Hofierka J. A new GIS-based solar radiation model and its application to photovoltaic assessments. *Transactions in GIS* 2004; **8**(2): 175–190, ISBN: 13611682.
23. Huld T, Müller R, Gambardella A. A new solar radiation database for estimating PV performance in Europe and Africa. *Solar Energy* 2012; **86**(6): 1803–1815.
24. Šúri M, Huld TA, Dunlop ED, Ossenbrink HA. Potential of solar electricity generation in the European Union member states and candidate countries. *Solar Energy* 2007; **81**(10): 1295–1305, ISBN: 0038092X.
25. Perpiñán O, Lorenzo E, Castro MA. On the calculation of energy produced by a PV grid-connected system. *Progress in Photovoltaics: Research and Applications* 2007; **15**(3): 265–274, ISBN: 10627995.
26. Perpiñán O, Lorenzo E, Castro MA, Eyra R. On the complexity of radiation models for PV energy production calculation. *Solar Energy* 2008; **82**(2): 125–131, ISBN: 0038092X.
27. Gordon JM, Wenger HJ. Central-station solar photovoltaic systems: field layout, tracker, and array geometry sensitivity studies. *Solar Energy* 1991; **46**(4): 211–217.
28. Lorenzo E, Pérez M, Ezpeleta A, Acedo J. Design of tracking photovoltaic systems with a single vertical axis. *Progress in Photovoltaics: Research and Applications* 2002; **10**(8): 533–543.

29. Perpiñán O, Lorenzo E, Castro MA, Eyras R. Energy payback time of grid connected PV systems: comparison between tracking and fixed systems. *Progress in Photovoltaics: Research and Applications* 2009; **17**(2): 137–147, ISBN: 10 627 995.
30. Real Decreto Ley 14/2010, de 23 de diciembre, por el que se establecen medidas urgentes para la corrección del déficit tarifario del sector eléctrico, Gobierno de España, Diciembre 2010.
31. Cruz-Peragón F, Casanova-Peláez PJ, Díaz FA, López-García R, Palomar JM. An approach to evaluate the energy advantage of two axes solar tracking systems in Spain. *Applied Energy* 2011; **88**(12): 5 131–5 142.
32. Lopez D, Muñoz R, Valero S, Senabre C. Analysis of a ground-mounted double axis photovoltaic installation in Spain. In *International Conference on Renewable Energies and Power Quality (ICREPQ11)*, Vol. 1, Las Palmas de Gran Canaria, Spain, 2010; 1–4. ISSN: 2172-038X.
33. Real Decreto 1578/2008, de 26 de septiembre, de retribución de la actividad de producción de energía eléctrica mediante tecnología solar fotovoltaica para instalaciones posteriores a la fecha límite de mantenimiento de la retribución del Real Decreto 661/2007, de 25 de mayo, para dicha tecnología, Gobierno de España, Septiembre 2008.